Emulating Dynamic Radio Channels for Radiated Testing of Massive MIMO Devices

Pekka Kyösti[1,2], Lassi Hentilä[1], Jukka Kyröläinen[1], Fengchun Zhang[3], Wei Fan[3], Matti Latva-aho[2]
[1]Keysight Technologies Finland oy, Oulu, Finland, firstname.lastname@keysight.com
[2]University of Oulu, CWC, Oulu, Finland, firstname.lastname@oulu.fi
[3]Department of Electronic Systems, Aalborg University, Denmark, firstname.lastname@es.aau.dk

***Abstract*—This paper discusses a multi-probe anechoic chamber setup, capable of reconstructing non-stationary radio propagation environments for testing of millimetre wave and massive Multiple-Input-Multiple-Output devices. The test setup is aimed for evaluation of end to end performance of devices, including hybrid beamforming operations of antenna arrays and base band processing, in highly time variant channel conditions. In this work we present simulated comparison of an ideal reference radio channel model and corresponding model implemented with limited resources of multi-probe anechoic chamber components. We give a qualitative analysis of the results with non-line of sight channel models, without quantitative evaluation. The example device under test is a 8×8 planar array with half wavelength inter-element spacing.**

***Index Terms*—Massive MIMO; performance evaluation; over the air testing; multi-probe anechoic chamber setup; mm-wave.**

I. Introduction

Currently new wireless telecommunication system, commonly called fifth generation (5G), is in standardization phase. Both base station (BS) and user equipment (UE) type of devices are actively developed, though any commercial products are not available yet. Characteristic to the devices is utilization of larger antenna arrays as compared to legacy 4G tranceivers. At sub 6 GHz frequencies massive Multiple-Input-Multiple-Output (MIMO) can be used for spectral efficiency in highly loaded cells through multi-user MIMO operations [1]. At millimetre wave (mm-wave) frequencies, antenna arrays are used for improving link budget, to compensate the severe path loss inherent to the frequency band and the high noise power due to wide bandwidths [1]. At mm-wave frequencies even UEs must rely on beamforming, as omni-directional antennas cannot provide high enough signal to interference plus noise power ratio (SINR).

At least the first devices operating at 28 GHz frequency area are expected to use the hybrid beamforming in their array operations. With the current technology each of the tens or hundreds of antenna elements may not be supported by separate radio frequency (RF) chains. In hybrid beamforming the arrays may be connected to a base band unit by only a small number of RF chains. The physical antenna elements are divided to sub-arrays and the elements within a sub-array are combined to a single RF port by an analog beamformer (weighting matrix). The matrix enables composing a predefined set of fixed antenna beams [2]. The analog beamformer, of each RF port, supports for a number of predefined beam shapes. Beam patterns are designed such that the full set of fixed beams cover the angular sector of interest. Both link ends are first expected to find the optimal beams in the link establishment procedure and then to continuously align the beams in the time-variant radio channel conditions, e.g., due to mobility in one or both ends. Given this, the beam allocation and the beam alignment are crucial operations to be tested.

In 4G and previous generations, BSs have been tested separately for RF performance and separately for radio resource management (RRM) and link performances in fading channels. The latter testing has been done in a conducted manner with coaxial cable connection between the device under test (DUT) and the test equipment. For testing of 4G UE the over the air (OTA) methods have been under research for many years and are already mature and in commercial use. The MPAC method [3] has been standardized in CTIA [4] and 3GPP [5], with some refinement still ongoing in 3GPP. Now, with large arrays and analog/hybrid beamforming, both the conducted testing and the reverberation chamber (RC) [6] or radiated two-stage (RTS) [7] based OTA methods are problematic in fading testing, as concluded in [8] and [9], [10].

The multi-probe anechoic chamber (MPAC) OTA techniques for massive MIMO or mm-wave device evaluations have been discussed in the literature [9]–[15]. The required number of probes of plane wave synthesis and prefaded signals synthesis methods are analyzed in [11] for two-dimensional (2D) circular probe configurations. Preliminary investigations on probe configurations and range lengths are reported in [12], with the main focus on precision of reconstructing an individual multi-path cluster. A sectored 3D probe configuration for massive MIMO testing with simulation results for the minimal physical dimensions of the setup are presented in [14]. Work on the physical dimensions assessment was continued in [9], with few new metrics and with the focus on 28 GHz frequency. Physical setup dimensions, probe configurations, and suitable channel models are discussed in [13]. Simulations were performed with 2D probe configurations with two 3GPP channel model scenarios (SCME UMi and UMa). A thorough description of sectored MPAC method is given in [10]. The current contribution continues the work and simulates reconstruction of a dynamic radio channel in OTA emulation. The principle was originally defined in [10], but no simulations were conducted.

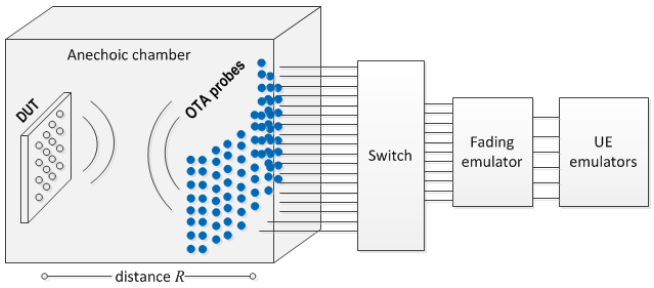

Fig. 1. Sectored MPAC setup [10].

It is expected that realistic end-to-end performance evaluation of mm-wave and massive MIMO devices in dynamic channel conditions is important for a number of reasons. Firstly, antenna arrays together with beamformers are essential parts of devices at mm-wave frequencies and the beamforming operation is essential in the link establishment procedure. Thus exclusion of the physical antennas from the performance testing might be harmful. The adaptive beamforming operation itself makes the radio channel highly dynamic. Secondly, at mm-wave frequencies the link distances may be short and even small motion may change the spatial structure of the propagation channel. Thirdly, the path gains are very sensitive to blockage by the user or other obstacles. This results to fast changes of power levels observed by different multi-path components.

II. MPAC SETUP

The sectored MPAC setup is illustrated in Fig. 1. It contains anechoic chamber, N probe antennas in a three-dimensional (3D) constellation covering a sector of azimuth and elevation angles, a fading channel emulator (CE) with K ports, a switch system connecting CE ports to probes, and a BS or UE emulator. The setup, its components and operations are described in [9], [10], [13], [14]. We leave details to be found from these references and present here only the high level functions. Transmitted signals of BS/UE emulator are modified within CE by channel transfer functions determined based on the channel model and the MPAC configuration. Then the faded signals are radiated towards the DUT by OTA probes within the anechoic chamber. In case of bi-directional fading emulation, the signals transmitted by the DUT are received by probes and routed through CE to the BS/UE emulator.

It is expected that probes, especially at mm-wave frequencies, are cheaper compared with the cost of CE resources. Thus, it is beneficial to use a switch to connect only the optimal sub-set of probes to the CE. A fixed sub-set for wide sense stationary (WSS) channels and a time-variant switching pattern for dynamic channels is determined as a pre-processing based on the given channel model. The switching is performed prior to the emulation in the static case and real time, i.e. during the emulation, in the dynamic case.

A. Determination of probe weights

In order to reconstruct the target power angular spectrum (PAS) within the test zone, each cluster of the target channel model is mapped to the set of active probes. The mapping is performed by routing the fading signals of a cluster to each active probe and by setting amplitude weights to the probes. In [10] was proposed to determine the weights with numerical optimization based on spatial correlation function similarly to previous 4G OTA systems [3]. With dynamic channel models the target PAS is time-variant and the weights must be updated frequently. Thus the method of weight calculation should be computationally fast. In the following we describe an effective method aiming to minimize the deviation of the target PAS and the PAS reconstructed by the OTA setup, as observable by the assumed DUT array.

The test zone is specified by a planar DUT array with certain assumed geometry. The target spatial covariance matrix is

$$\mathbf{R}_r = \oint \mathbf{a}(\Omega) P_r(\Omega) \mathbf{a}^H(\Omega) d\Omega \in \mathbb{C}^{M \times M}, \tag{1}$$

where $\mathbf{a}^H(\Omega) \in \mathbb{C}^{M \times 1}$ is the steering vector of DUT array to direction Ω, M is the number of DUT elements, and $P_r(\Omega)$ is the PAS specified by the target model. As described in [10], the target PAS estimated by DUT with Bartlett beamformer is

$$\hat{P}_r(\Omega) = \mathbf{a}^H(\Omega) \mathbf{R}_r \mathbf{a}(\Omega). \tag{2}$$

Next we compose a steering matrix $\mathbf{A} = [\mathbf{a}(\Omega_1) \dots \mathbf{a}(\Omega_K)] \in \mathbb{C}^{M \times K}$ of DUT array to OTA probe directions Ω_k, $k = 1, \dots, K$. The following matrix resembles the PAS estimate of eq. (2) to directions of K probes

$$\hat{\mathbf{P}}_o = \mathbf{A}^H \mathbf{R}_r \mathbf{A} \in \mathbb{C}^{K \times K}. \tag{3}$$

Now the amplitude weight vector for K probes is determined simply as

$$\mathbf{\Gamma} = \sqrt{|\mathrm{diag}(\hat{\mathbf{P}}_o)|} \in \mathbb{R}^{K \times 1}, \tag{4}$$

where $\mathrm{diag}()$ is an operator picking diagonal elements of a matrix into column vector.

The defined weight calculation method is computationally effective, as it does not contain any numerical optimization. The method is used in simulations described in following sections. An example illustration of resulting power weights over an emulation time period is shown in Fig. 2 (bottom).

III. SIMULATION SETTINGS

We have performed an example simulation with an MPAC setup, a DUT, and a dynamic channel model. Purpose of the simulation is to evaluate how the system operates and to perform visual (qualitative) comparison of resulting performance and accuracy.

DUT is 8×8 planar array of in total 64 elements. Spacing of elements is half wavelength both in horizontal and vertical

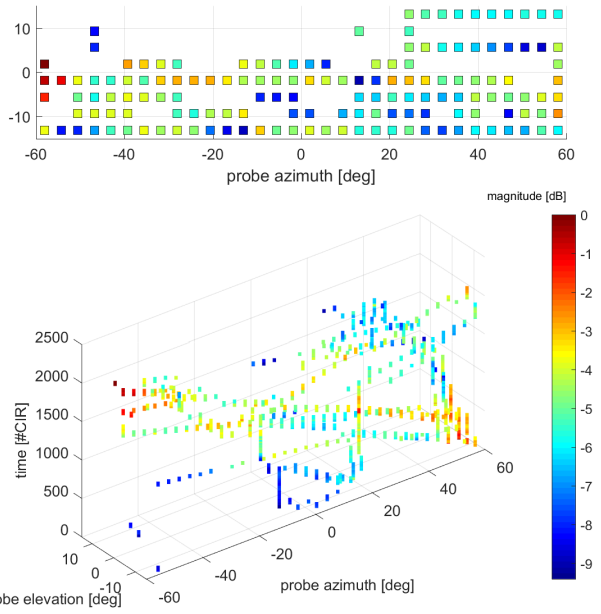

Fig. 2. Selected probes (top) and power weights of probes (bottom) over emulation time.

direction. Elements are isotropic and vertically (single) polarized. In practise the polarization dimension is not investigated in this study, as the spatial/angular structure is in the focus. At 28 GHz frequency the array is approximately 4 by 4 cm in physical size. DUT could represent, e.g., a single sub-array of a BS.

The reference channel model is a geometry-based stochastic channel model (GSCM) urban micro-cellular line of sight (LOS) scenario. The procedure of generating dynamic channel parameters is as follows. At first, three randomly generated sets of propagation parameters, like path delays, angles, and average powers, are drawn from probability distributions specified by the GSCM. The three sets represent three way-points of a route. Then, the propagation parameters are linearly interpolated for the locations (route) in between the way-points. Finally, fast fading is generated according to the principles of the GSCM. A detailed description of the method is given in [16]. We want to emphasize, that the probe selection and weighting, mentioned in the previous section, are not based on the fast fading power levels but on the interpolated (ensemble) average powers of paths.

The resulting dynamic channel conditions are illustrated, with respect to azimuth angle of departure (AoD), in Fig. 3. There the linearly varying AoDs over time are visible together with the temporal fading patterns. The number of clusters is 16. Ricean K-factors are 9, 15 and 7 dB in the three subsequent "locations" at time instants of 0, 1122 and 2318, respectively (see time axis of Fig. 3). From start to end of the dynamic reference channel model, the AoD of the LOS path moves linearly from +21° to -22°, while the corresponding elevation angle of departure (EoD) remains 0°. Other fading paths have a wide range of AoDs and EoDs, as can be partially read from Fig 3. An UE with single vertically polarized dipole antenna was assumed for the other link end.

The simulated MPAC setup contains probes with 3.75° spacing, in a sector of 120° in azimuth and 30° in elevation. The total number of probes is as high as 512. At total eight probes are active simultaneously, i.e. eight ports of a CE are used. The probes are selected independently for each time instant, based on the target PAS, as described in [10]. In this study we assume that the switching configuration is completely free and the switching can be performed for each considered time instant without any distortions. These assumptions and the number of probes may be too idealistic for a practical setup. It is a topic for further study to investigate more practical limitations. Range length $R = 2$ m in the simulation.

The radio channels from the other link end (UE) to the DUT array are calculated for both the reference model case and for the OTA case. For the reference case, the channel impulse response (CIR) matrices $\mathbf{H}_{\text{ref}}(t, f)$ are determined as specified for the GSCMs, e.g., in [17]. In the latter the physical probe and DUT antenna locations are used to determine transfer functions from probes to the DUT. The channel coefficients are finally composed as a $N \times M$ (64×1) vector of CIRs from UE to DUT elements, for 2318 time instants.

The transfer matrix $\mathbf{H}_{\text{ota}}(t, f) \in \mathbb{C}^{N \times M}$, containing predominantly the temporal and the frequency fading components of the channel model, is defined as

$$\mathbf{H}_{\text{ota}}(t,f) = \mathbf{F}(f) \left(\sum_{l=1}^{L} \text{diag}\left(\mathbf{\Gamma}_l(t)\right) \mathbf{G}_{id} \begin{bmatrix} \alpha_{l,k}^{\theta\theta}(t,f) & \alpha_{l,k}^{\theta\phi}(t,f) \\ \alpha_{l,k}^{\phi\theta}(t,f) & \alpha_{l,k}^{\phi\phi}(t,f) \end{bmatrix} \mathbf{G}_{tx}^{T}\left(t, \mathbf{k}_l^{tx}(t)\right) \right), \tag{5}$$

where $\mathbf{F}(f) \in \mathbb{C}^{N \times K}$ is the transfer matrix from K probes to N DUT antennas, $\mathbf{\Gamma}_l(t)$ from eq. (4) is composed of weights of K probes for the lth cluster, $\mathbf{G}_{id}$ is $K \times 2$ ideal polarimetric antenna pattern matrix of OTA probes with entries $\in \{0, 1\}$, coefficients α_l^{ab} are the complex channel gains of path l and probe k for transmitted polarization b and received polarization a, $\mathbf{G}_{tx} \in \mathbb{C}^{M \times 2}$ is the polarimetric antenna pattern vector of θ and ϕ polarizations for Tx antenna arrays, and wave vector $\mathbf{k}_l^{tx}$ defines both the frequency and the direction of arrival/departure to sample the radiation patterns of Tx antennas. The above-mentioned sequence of 64×1 CIR matrices is obtained by taking Fourier transform of eq. (5) over frequency domain.

IV. Simulation Results

As described earlier, the first step is to find the optimal sub-set of active probes for each time instant and then to find power weights for the probes. In Fig. 2 (top) is shown the selected probes over all time instants in their azimuth/elevation positions. The bottom figure illustrates instantaneous probe allocations, together with the weight magnitudes. Horizontal

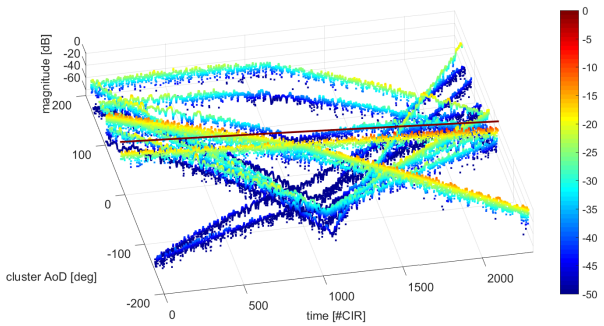

Fig. 3. Fading paths of the reference channel model.

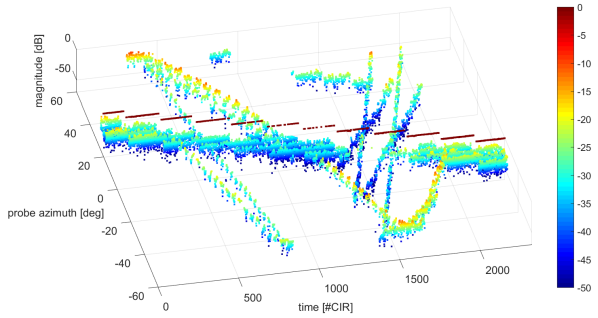

Fig. 4. Angular fading reconstructed by the OTA setup.

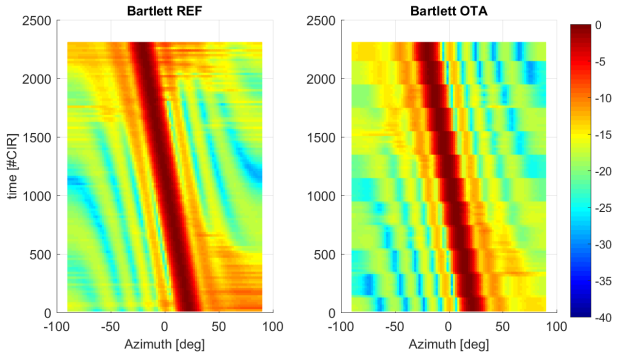

Fig. 5. Estimated marginal azimuth power distribution for the reference model (left) OTA (right).

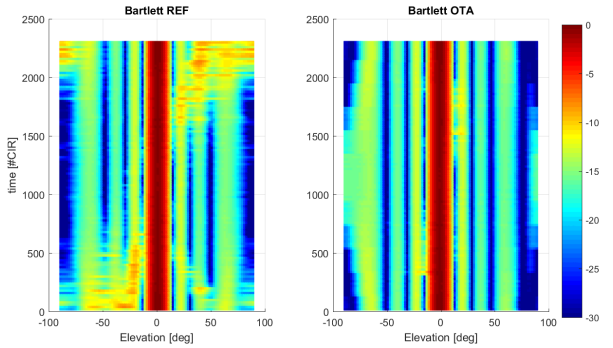

Fig. 6. Estimated marginal elevation power distribution for the reference model (left) OTA (right).

axes denote the elevation and azimuth angles of probes, while the vertical axis presents time. The magnitude of probe weights per time instant, i.e., elements of vector $\sum_l \mathbf{\Gamma}_l(t)$, are colour coded in decibel scale. At each time instant, i.e., at each vertical slice of the figure, there are only eight active probes and correspondingly eight coloured markers. The top figure is a top view of the bottom figure. The top view shows which probes were active and which remained unused during the emulation.

The resulting fading in the OTA case in time/probe azimuth angle plot is depicted in Fig. 4. This is, to some extent, comparable with the reference model of Fig. 3. It is worth of noticing that the AoD axes of the figures have different scales and also that many clusters of the reference model are outside of the probe sector at some points of time. The main propagation paths of Fig. 3 and their time evolution, especially the LOS path, are identifiable in Fig. 4. The straight dark red line in Fig. 3 and the dashed line in Fig. 4 represent the LOS path. In OTA case the weakest paths are not reconstructed in their true directions, as the number of simultaneously active probes is limited to eight in the simulated case.

Another view to the comparison is the estimated PAS as observed by the DUT through Bartlett beamforming. These comparisons for joint azimuth-elevation spectra, together with a quantitative assessment, for static models are presented in [10]. For dynamic models the time dimension must be considered too. We have estimated PASs as defined in [10] for consecutive time segments of 20 samples and calculated marginal azimuth and elevation PASs as shown in Figures 5 and 6, respectively. From Fig. 5 we can observe the quantized evolution of azimuth spectrum. Of course, the sparser the spacing of probes the rougher quantization results. Despite the quantization the estimated spectra are rather similar. In Fig. 6 (left) the power component evolving from negative to positive elevation is missing in the OTA case (right). This must result from a cluster that is outside of the probe sector most of the time.

The final evaluation is done with a metric of beam allocation distributions, defined in detail in [10]. There is assumed that the DUT has a code book of fixed beams and for each time instant a single beam is allocated to the direction offering highest power. Now in Fig. 7 is depicted fixed beam directions and their probabilities for both the reference and OTA cases. This metric is directly usable in dynamic cases, as the time variation is naturally embedded in the probability distribution histogram. As we can observe, the beam allocation distribution of the reference model is well reconstructed by the simulated OTA setup. The quantitative metrics of Beam statistical distance and Beam peak distance (see definitions in [10]) get values 0.08 and 0.09, respectively.

The discussed three views to the emulated dynamic channels all describe the same system, but they have also some clear differences. The first view of Fig. 3 and 4 demonstrate the

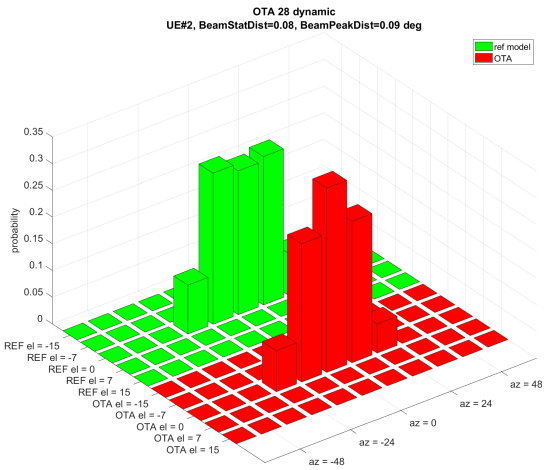

Fig. 7. Probability distribution of beam allocations by the DUT.

instantaneous channel coefficients in angular domain, without considering the DUT or the test zone dimensions at all. The second view of Fig. 5 and 6 takes into account some DUT characteristics and is closer to a practical interest. If the devices to be tested use analog beamforming with fixed code books, the third view of beam allocation distributions (Fig. 7) is closest to practical functionality of this kind of devices. If the channel model was static LOS channel the beam allocations occurred in a single beam direction only.

V. Conclusions

We have discussed a sectored MPAC OTA setup targeted for testing of mm-wave and massive MIMO devices. Dynamic channel models and dynamic test conditions should be seriously considered for testing of 5G devices, as the real propagation conditions are expected to be non-WSS at mm-wave frequencies. Moreover, the beamforming operations are essential already for the link establishment. We have sketched the process of reconstructing dynamic channel conditions with the OTA setup.

Further, we have performed first simulations demonstrating the capability of emulating dynamic channel models. Three different subjects were compared between the reference model and the OTA scenario: instantaneous fading coefficients in azimuthal space, marginal PASs over time segments, and probability distributions of fixed beam allocations. All evaluations give encouraging results on the capability of emulating dynamic channels with limited MPAC hardware resources.

Future work is needed to evaluate impacts of different probe configurations, range lengths, and numbers of CE resources. Also different practical switching constraints must be considered. Further simulations could be performed with quantitative metrics. The beam allocation metrics are applicable as such. The time-variant PASs could be interpreted as 3D probability distributions over time and space angle. Then the total variation distance could be calculated between the reference and the OTA distribution, similarly as for the static case in [10].

Acknowledgment

The part of this research performed at University of Oulu has been supported by Finnish Funding Agency for Technology and Innovation (Tekes), Nokia, Bittium, MediaTek, Kyynel, and Keysight Technologies Finland.

References

[1] E. G. Larsson, O. Edfors, F. Tufvesson, and T. L. Marzetta, "Massive MIMO for next generation wireless systems," *IEEE Communications Magazine*, vol. 52, no. 2, pp. 186–195, February 2014.

[2] Verizon, "Air interface working group; Verizon 5th generation radio access; physical layer procedures," Verizon 5G TF, Tech. Rep. TS V5G.213 v1.0, June 2016.

[3] P. Kyösti, T. Jämsä, and J.-P. Nuutinen, "Channel modelling for multiprobe over-the-air MIMO testing," *International Journal of Antennas and Propagation*, vol. 2012, 2012.

[4] CTIA, "Test Plan for 2x2 Downlink MIMO and Transmit Diversity Over-the-Air Performance," CTIA Certification, Tech. Rep. Version 1.0, August 2015.

[5] RP-160603, "Radiated performance requirements for the verification of multi-antenna reception of UEs," 3GPP, Tech. Rep., March 2016.

[6] X. Chen, "Throughput modeling and measurement in an isotropic-scattering reverberation chamber," *IEEE Transactions on Antennas and Propagation*, vol. 62, no. 4, pp. 2130–2139, April 2014.

[7] W. Yu, Y. Qi, K. Liu, Y. Xu, and J. Fan, "Radiated two-stage method for LTE MIMO user equipment performance evaluation," *IEEE Transactions on Electromagnetic Compatibility*, vol. 56, no. 6, pp. 1691–1696, Dec 2014.

[8] M. Rumney, P. Cain, T. Barratt, A. L. Freire, W. Yuan, E. Mellios, and M. Beach, "Testing 5G: evolution or revolution?" in *Radio Propagation and Technologies for 5G (2016)*, October 2016, pp. 1–9.

[9] P. Kyösti, J. Kyröläinen, and W. Fan, "Assessing measurement distances for OTA testing of massive MIMO base station at 28 GHz," in *2017 11th European Conference on Antennas and Propagation (EUCAP)*, March 2017, pp. 3679–3683.

[10] P. Kyösti, L. Hentilä, W. Fan, J. Lehtomäki, and M. Latva-aho, "On radiated performance evaluation of massive MIMO devices in multi-probe anechoic chamber OTA setups," *IEEE Transactions on Antennas and Propagation*, 2017, submitted 5/2017.

[11] A. Khatun, K. Haneda, M. Heino, L. Li, P. Kyösti, and R. Tian, "Feasibility of multi-probe over-the-air antenna test methods for frequencies above 6 GHz," in *2015 Loughborough Antennas Propagation Conference (LAPC)*, Nov 2015, pp. 1–5.

[12] D. Reed, A. Rodriguez-Herrera, and R. Borsato, "Measuring massive MIMO array systems using over the air techniques," in *2017 11th European Conference on Antennas and Propagation (EUCAP)*, March 2017, pp. 3663–3667.

[13] W. Fan, I. Carton, P. Kyösti, A. Karstensen, T. Jämsä, M. Gustafsson, and G. F. Pedersen, "A step toward 5G in 2020: Low-cost OTA performance evaluation of massive MIMO base stations," *IEEE Antennas and Propagation Magazine*, vol. 59, no. 1, pp. 38–47, Feb 2017.

[14] P. Kyösti, W. Fan, G. F. Pedersen, and M. Latva-aho, "On dimensions of OTA setups for massive MIMO base stations radiated testing," *IEEE Access*, vol. PP, no. 99, pp. 1–1, 2016.

[15] W. A. T. Kotterman, C. Schirmer, M. H. Landmann, and G. Del Galdo, "New challenges in over-the-air testing," in *2017 11th European Conference on Antennas and Propagation (EUCAP)*, March 2017, pp. 3676–3678.

[16] L. Hentilä, P. Kyösti, and P. Heino, "Evaluation of beam forming and multi antenna techniques in non-stationary propagation scenarios with HW emulator," in *2012 International ITG Workshop on Smart Antennas (WSA)*, March 2012, pp. 347–351.

[17] TR 38.901, "Study on channel model for frequencies from 0.5 to 100 GHz," 3GPP, Tech. Rep. V14.1.1, July 2017.